Volume 17 Number 1 1989 Nucleic Acids Research

The interaction of *E.coli* integration host factor and λ *cos* DNA: multiple complex formation and protein-induced bending

Linda D.Kosturko, Elisabeth Daub[1+] and Helios Murialdo[1]

Department of Molecular Biology and Biochemistry, Hall-Atwater Laboratory, Wesleyan University, Middletown, CT 06457, USA and [1]Department of Medical Genetics, Medical Sciences Building, University of Toronto, Toronto, Ontario M5S 1A8, Canada

Received August 17, 1988; Revised and Accepted November 22, 1988

ABSTRACT

The interaction of *E. coli's* Integration Host Factor (IHF) with fragments of lambda DNA containing the *cos* site has been studied by gel-mobility retardation and electron microscopy. The *cos* fragment used in the mobility assays is 398 bp and spans a region from 48,298 to 194 on the lambda chromosome. Several different complexes of IHF with this fragment can be distinguished by their differential mobility on polyacrylamide gels. Relative band intensities indicate that the formation of a complex between IHF and this DNA fragment has an equilibrium binding constant of the same magnitude as DNA fragments containing lambda's *attP* site. Gel-mobility retardation and electron microscopy have been employed to show that IHF sharply bends DNA near *cos* and to map the bending site. The protein-induced bend is near an intrinsic bend due to DNA sequence. The position of the bend suggests that IHF's role in lambda DNA packaging may be the enhancement of terminase binding/*cos* cutting by manipulating DNA structure.

INTRODUCTION

As part of its reproductive cycle, bacteriophage lambda incorporates the viral DNA chromosome into a preformed protein shell called a prohead. This process is called DNA encapsidation (for a review see 1). The virally-encoded protein which recognizes the lambda DNA packaging signal to initiate the process is terminase (2). The signal on DNA is called *cos* and consists of *cosN*, the nicking site, and *cosB*, the site where terminase initially binds (3).

Purified terminase cannot cut *cos* in the absence of host proteins (4). Two such proteins are the terminase host factor (THF) and integration host factor (IHF) (5). THF is a small, basic protein which binds lambda DNA near *cos* (6).

IHF is a basic, heterodimeric protein of 21,800 kilodalton, encoded by the *himA* and *himD* genes of *E. coli* (7, for a review, see 8). It is a sequence-specific DNA-binding protein, which is essential for lambda site-specific recombination into and out of the *E. coli* chromosome (9). In addition IHF has been shown to participate in many other cellular processes,such as the initiation of replication (10,11), transposition (12) and the regulation of gene expression (13,14,15).

In site-specific recombination, IHF binds to three sites near *attP* and assists in the formation of a nucleoprotein complex which guarantees precision of the endonucleolytic cleavages (16,17). Using gel-mobility retardation, IHF has been shown to bend DNA at two of these sites (18) and also at the pSC101 origin of replication (11).

The sequence of lambda encompassing *cos* (Fig. 1) contains several near-matches (19) to the

IHF consensus sequence, PyAANNNNTTGATa/t (20,21), and many of these sites (I1,I2,I3, and I4) can be protected by IHF from DNase nicking (22). The IHF footprints near *cos* are interspersed among footprints (R sites) of the gp*Nu1* subunit of terminase (23). This array of interspersed DNA binding motifs is analogous to the situation at *attP* with IHF and other proteins.

The importance of IHF in terminase action has been demonstrated in several ways. In *recA* deficient cells, terminase nicks sites in the bacterial chromosome, but mutations in either *him*A or *himD* allow cells to survive this lethal effect (24).

Although wild type lambda grows in IHF deficient cells, the burst size is only 25% of that in wild type cells (19,25). A mutant of lambda, *cos* 154, is IHF-dependent for growth. The mutation is a single base pair substitution within one of the sequences footprinted by gp*Nu1* (19). Another IHF-dependent mutant, *cos* 59, is a deletion of three base pairs in the IHF-binding site 12 (25), that is, outside the terminase-binding sites. IHF-independent pseudorevertants of *cos* 59 were found to be point mutations in the *Nu1* subunit of terminase (26). Exactly the same mutation in *Nu1* was found in a λ mutant selected for its ability to grow on *E. coli himA gyrB* at 42°C, conditions under which λ wild type does not grow (27).

Thus, the combined genetic and biochemical data suggest that IHF plays a role in lambda DNA packaging either by altering the DNA structure around *cos* or by establishing protein: protein interactions with terminase, or both.

To investigate further the role of IHF in lambda DNA packaging, we have studied the binding of IHF to cloned fragments of lambda DNA using gel electrophoresis (28,29) and electron microscopy (30). Our data suggest that the binding of IHF to *cos* DNA is complex and dependent on both buffer composition and temperature. In addition we found that IHF sharply bends DNA near *cos* at I1 (Fig.1) and that the bend lies close to a sequence-induced bend in the DNA fragment.

MATERIALS AND METHODS

Cells and Plasmids

Cells were grown on Luria-Bertani medium at 37°C. Three plasmids have been used to prepare DNA fragments for the experiments reported here. Plasmids pBW10 and pLK1010 were maintained in *E. coli* GM2929, a *dam-, dcm-* strain constructed by Martin Marinus; pWP14 was maintained in JM101 (31). pBW10, a construct from Michael Feiss (3), is a derivative of pACYC184 and contains 700 bp of lambda DNA (32), spanning the *cos* site, from a *Bcl*I site at coordinate 47,942 to an *Eco*RI site resulting from a single base substitution at position 194. Cutting pBW10 with *Eco*RI and *Hind*II produces a fragment of 398 bp which spans the *cos* site.

A plasmid containing a tandem duplication of this 398 bp fragment pLK1010, constructed by ligating *Eco*RI linkers to the *Hind*II terminus and cloning the resulting fragment into the *Eco*RI-cut pBW10. The clone was identified by its size and its ability to produce the 398 bp fragment when the plasmid was cut by any restriction enzyme which cut the original fragment at a single site.

The DNA fragment used for electron microscopy was prepared from the plasmid pWP14 (33).

This plasmid was constructed by inserting the *cos*containing *Hinc* II fragment of bacteriophage lambda, from lambda coordinate 48,298 to 199, into the *Hind*II site of pUC9. A fragment containing *cos* was excised from pWP14 by digestion with *Pvu*II.

Preparation of DNA

Plasmids were released from cells by boiling after Triton-lysozyme lysis (34) or by means of an alkaline extraction procedure (35). They were purified by ethidium bromide-cesium chloride density gradient centrifugation (34). To prepare DNA fragments, plasmid DNA was cut with the appropriate restriction enzymes, under conditions recommended by the manufacturer (either Bethesda Research Laboratory, Boehringer Mannheim or New England Biolabs). The fragments in the digest were separated by electrophoresis in agarose (SeaKem, GTG, FMC Corp.). Bands containing the fragments of interest were cut from the gel. For binding studies, the DNA was eluted from the gel slices into a sink of 160µl of saturated ammonium acetate, at 100 V, for 15 minutes using an IBI EA electroeluter. The DNA was further purified by phenol extraction and ethanol precipitation to produce a translucent, salt-free DNA pellet. For electron microscopy, the fragment was isolated using NA-45 (DEAE) membrane (Schleicher and Schuell, Inc.). The 704 bp *Pvu* II fragment was further purified by Elutip-d elution (Schleicher and Schuell, Inc.) and ethanol precipitation.

Labelling DNA Fragments

DNA fragments were labelled at their 5' ends using T4 polynucleotide kinase (PL Biochemicals) and γ-^{32}P-dATP (New England Nuclear) using the procedures for 5' protruding ends or blunt ends described in Maxam and Gilbert (36).

IHF Preparation

Integration Host Factor was purified from an overproducer strain constructed by Nash *et al.* (37) according to the author's recommendations. Protein for some experiments was purified in our laboratory and for others was a gift from Howard Nash. Regardless of source, the IHF was 95% pure with no contamination of HU, a histone-like protein of *E. coli.*

IHF:DNA Binding Reaction

Two different reaction buffers were used. The spermidine buffer system combined 16 µl of DNA in 41.4 mM Tris, pH 8.3, 58 mM KCl, 0.8 mM Na_2EDTA, 6.3 mM spermidine-HCl, 1.25 mg/ml bovine serum albumin (BSA) with 4 µl of serially diluted IHF in 50mM Tris, pH 7.4, 800 mM KCl, 30mM Na_2HPO_4, 9mM KH_2P0_4, 10%glycerol. This combination reproduces the binding buffer first described for IHF (7). The magnesium buffer system combined 10 µl of DNA in 52 mM Tris, pH 7.4, 70 mM KCl, 1.1 mM Na_2EDTA, 1.0 mM β-mercaptoethanol, 7 mM $MgCl_2$, 200 µg/ml BSA, 10% glycerine, with 10 µl of serially diluted IHF in the same buffer. This buffer is essentially the same as described for DNase footprinting of IHF sites (20), except for the absence of calcium. Using either system, the DNA concentration in the reaction mixture was 0.5 to 5.0 nM, and the IHF concentration ranged from 0.01nM to 500 nM.

Before incubation, protein and DNA were separately maintained at 0°C. Solutions were carefully mixed by gentle agitation to avoid foaming. The mixtures were incubated at 25°C for 20 or 30 minutes and immediately loaded, without any addition of dye or weighting solution, onto a polyacrylamide gel, with the current on to rapidly trap protein-DNA complexes within the matrix of the gel.

Gel Electrophoresis

The analysis of protein: DNA complexes by polyacrylamide gel electrophoresis was done on 5% gels (29:1, acrylamide:bis-acrylamide) in a modified TBE buffer (50 mM Tris-base, 120 mM boric acid, 2 mM Na_2EDTA, pH 8.2) for a final pH of 8.1, measured at either 25°C or 4°C.

Gels were either 28 x 10 x .14 cm or 13.5 x 10 x .14 cm and ran at constant power at 2-3 watts. Following electrophoresis, gels with labelled DNA fragments were transferred to Whatman #1paper and dried at 60°C *in vacuo*. For autoradiography Kodak XAR-5 film and Dupont Cronex lightening-plus intensifying screen were used. For quantitative measurements of band intensity,autoragraphic films were scanned with a Zeineh softlaser scanning densitometer, Model SLR-2D/1D.

Electron Microscopy

Copper grids (Veco, 400 mesh) were prepared following the technique of Williams (30). The grids were coated with polyvinal formal (formvar, JBS Scientific Inc.) and subsequently coated with carbon. The filmed grids were subjected to glow discharge at about 100 millitorr for 20-30 seconds. Polylysine (Sigma Chemical Corp., molecular weight of 3600), diluted to 1μg/ml in water, was placed on the grid (5 μl) for 30 seconds and removed by aspiration. The grids were allowed to dry before sample application.

The dilution buffer and incubation buffer used was 20 mM Bis-tris-propane (pH 7.2), 10 mM $MgCl_2$, 25 mM KCl and 15 mM β-mercaptoethanol. Mg++ is essential for DNA absorption to the grid. The DNA was diluted to 15 μg/ml in this buffer. The IHF preparation was diluted to 22 μg/ml. Equal volumes (about 5μl) of each DNA, IHF solution and buffer were mixed and allowed to sit at room temperature for 5 min. This corresponds to a molar ratio of DNA to IHF of about 1:20. The solution was diluted 10-fold further for absorption to the polylysine-treated grids. After a 5 min absorption period, the solution was aspirated off, and the grid was rinsed with 4 drops of distilled water. Uranyl acetate (5% in water) was applied for 15 sec and subsequently removed, followed by 3 more washes with a drop of water. The grids were lightly rotary shadowed with Pt/Pd wire (JBS Scientific, Inc.) at an angle of 10° and a source- to-sample distance of 10 cm. Electron microscopy was performed on a Hitachi H7000 electron micro- scope, with a primary nominal magnification of 40,000 X, using Kodak Electron Micrograph Film. The negatives were projected onto a screen so that total magnification was 532,000 X as determined with an electron micrograph with a crossed diffraction grating with 2,157 lines/mm. Individual DNA molecules were traced, and contour lengths were measured with a Numonics Digitizer.

RESULTS

Gel Mobility Retardation

The *cos* DNA fragment (Fig. 1) has several sites with near matches to the IHF consensus site (20, 21) that can be footprinted by IHF (22). A titration of this fragment with increasing amounts of IHF should produce multiple IHF-DNA complexes resolvable by gel electrophoresis. The relative mobility of these complexes would suggest the stoichiometry of IHF-DNA interaction under these conditions, while the relative band intensities would give the equilibrium binding constant for each complex. Fig. 2 shows an autoradiograph of such an experiment. Each lane

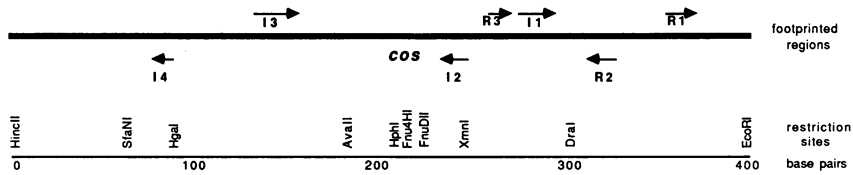

Figure 1: Diagram of the packaging region of lamda DNA.

The thick line represents the 398 bp fragment used in these experiments. The sequence cleaved by terminase to produce the cohesive ends of the lambda chromosome is indicated by *cos*. The sequences protected from nicking by DNase I by IHF and by the gp*Nu1* subunit of terminase are indicated by I1, I2, I3, and I4, and by R1, R2, and R3, respectively. The direction of the arrows and the position of the label, above or below the line, indicates the polarity of the consensus sequences within the protected site. The thin line below represents a restriction map of unique sites within the region. In the lambda chromosome, the *Hinc*II cut site is found just after base 48,298 while the *Eco*RI cut site corresponds to a cut just after position 194.

shows the complexes produced by a combination of end-labelled DNA, 1.1 nM, and increasing concentrations of IHF. The actual IHF concentrations in the mixtures ranged from 0.1 nM to 400 nM. For comparison, if one assumes that there were 1000 molecules of IHF per cell of *E. coli* (38), then the intracellular concentration of IHF would correspond to 1.5 μM. Under these conditions, three bands, A, B, and C, of lower mobility than free DNA were resolved by electrophoresis. Densitometry of three representative lanes from Fig. 2 more clearly distinguishes the three bands and the shift of DNA from one band to the other as the IHF concentration increases (Fig. 3). Complex formation is observed at IHF concentrations far below the concentration (45 nM) needed to protect the strongest IHF-binding site (I1) from nicking by DNase (22).

The sharpness of the bands indicates that the complexes seem to be stable over the six hours of electrophoresis. The mobility shift observed is greater from free DNA to A, than from either A to B or from B to C. This same pattern is seen for catabolite activator protein (CAP) binding to a *lac* promoter region with multiple specific binding sites (39).

The pattern of complexes formed is substantially the same using either the spermidine or the magnesium binding buffers. Although this experiment was run at 4°C, at 25°C, B and C are less sharp. Perhaps these complexes are more sensitive to temperature (data not shown).

The binding of IHF to *cos* DNA is sequence-specific. If IHF is added to a mixture of two DNA fragments, the IHF preferentially binds and retards the fragment containing matches to the IHF consensus binding site. Figure 4 shows the results of combining the 398 bp *cos* DNA fragment with the *Bam* HI - *Sal* I fragment of pBR322, which contains no IHF sites. At low IHF concentrations, the *cos* fragment is retarded, forming Complex A. As the IHF concentration is increased, higher order complexes are observed. At IHF concentrations where most of the *cos* fragment is bound, the pBR322 fragment begins to form non-specific complexes. Only at sufficiently high concentrations of IHF can non-specific binding engage all of the pBR322 fragment in a protein-DNA complex.

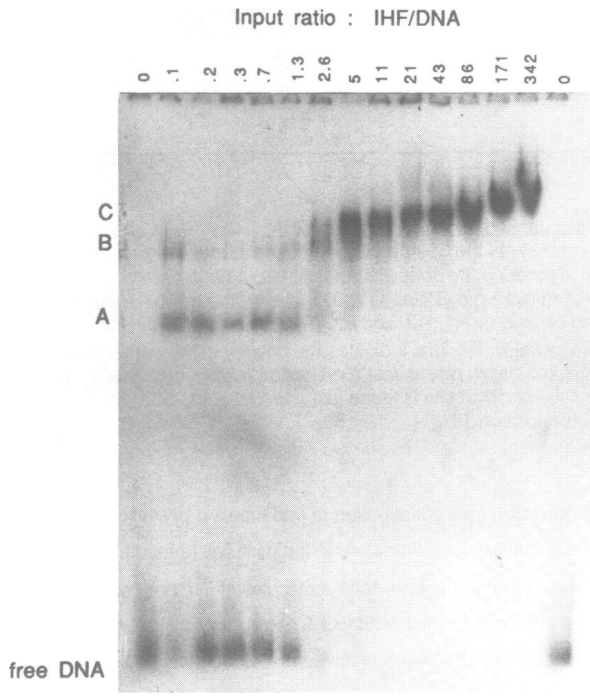

Figure 2: Titration of the *cos* DNA fragment by IHF binding.
The molar ratio of IHF to DNA in each mixture is indicated above the lane. The mobility of free DNA and of three IHF:DNA bands resolved by electrophoresis are indicated by the labels on the left. The polyacrylamide gel was run at 4°C.

To quantitate the specificity of binding, the free DNA bands were scanned by laser densitometry and the integrations were used to calculate the fraction of each DNA fragment bound to IHF in each mixture, relative to the total amount of DNA bound (Figure 5). Any non-specific binding would be expected to affect both fragments equally, but IHF would be expected to bind specifically only to the *cos* DNA. Specificity would be indicated by a preferential binding of IHF to the *cos* DNA fragment disproportionate to its representation in the input mixture of the two DNA fragments. At low IHF concentrations, the specificity ratio indicates a preference for *cos* DNA. At 20nM, when nearly all of the *cos* fragment is bound in IHF complexes, non-specific binding to the pBR322 fragment becomes significant. At 50 nM all DNA of both fragments is bound, and the specificity ratios converge at the proportion found in the input mixture of the two DNA fragments (1.00). Taken together, Figures 3 and 4 suggest that at concentrations of IHF sufficient to produce complex A and, perhaps, B, protein binding is sequence-specific. At higher IHF concentrations, complexes C and D may result from non-specific protein-DNA or from protein-protein interactions.

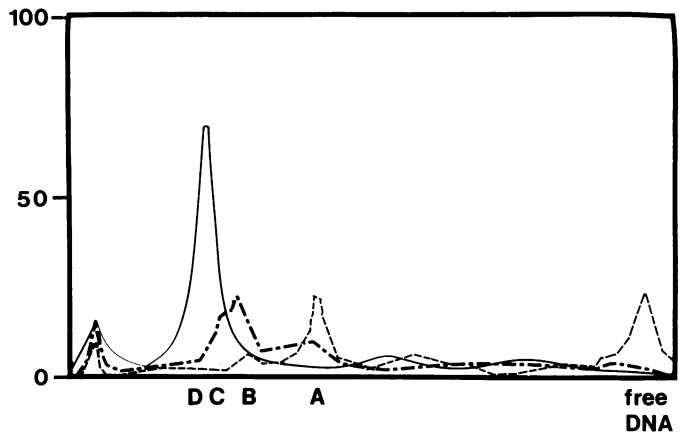

Figure 3: Densitometry of complex formation as a function of IHF concentration.
The overlapping of the three tracings shows the shift from free DNA to more slowly migrating bands (A, B, C, D) as the molar ratio of IHF to DNA is increased. The molar ratios of IHF to DNA shown are 0.2, dashed line; 2.6, alternating long-short dashes; 21, solid line.

In Fig. 2, at very low ratios of IHF to DNA, two bands, A and B, were observed, and the relative amount of each was not changed significantly over several dilutions of IHF. This pattern is also seen in CAP binding to a multi-site fragment where the use of labeled protein established that both bands were 1:1 complexes of protein and DNA. This result suggests that A and B complexes could result from IHF binding to different sites on the *cos* fragment, for instance to I1 and to the second strongest binding site, I2 (see Fig. 1).

If A represents a 1:1 complex of IHF to DNA, then B might represent a complex containing more than one IHF molecule bound per fragment. Using a densitometer to measure the fraction of DNA present in the three bands (free, A and B) for each mixture with an input ratio less that one, it is possible to calculate equilibrium binding constants for the formation of A and B (39). Although we have not extensively studied the kinetics of IHF interaction with *cos* DNA, we have increased the time of reaction by 50% without noticing an effect in the amount of DNA bound. The densitometric values were used to calculate the proportion of DNA in the complex.

The data can be modeled in several different ways. If we assume that both A and B are formed by one IHF molecule binding to one molecule of DNA and that A cannot directly convert to B, then A and B are both in equilibrium with free DNA and free IHF, where the free IHF is equal to the IHF added minus the portion bound to form A and B (39) as follows:

$$DNA + IHF \rightleftharpoons A$$

$$DNA + IHF \rightleftharpoons B$$

The log of the inverse of the equilibrium binding constant is equal to the x-intercept in a plot of the log [(DNA bound)/(DNA free)] versus the log [IHF free]. Using this model, we have calculated the binding

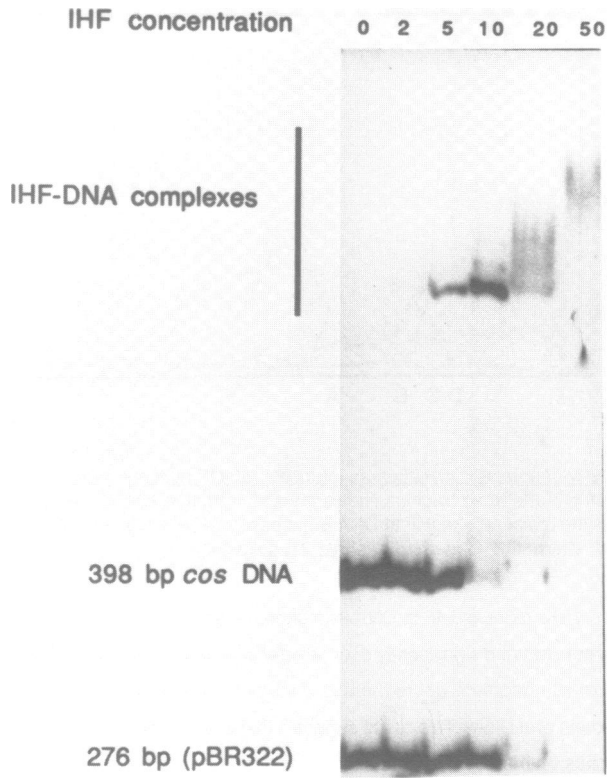

Figure 4: Competitive binding of IHF to two DNA fragments.
The 398 bp *cos* DNA fragment and the 276 bp *Bam H*1-*Sal*1 fragment from pBR322 were combined with various concentrations of IHF, and complexes were separated from the free DNA fragments by gel electrophoresis. The IHF concentrations shown are 2nM, 5nM, 10nM, 20nM and 50nM. At 2nM complex A is observed; at 5nM complex B appears. Higher order complexes are observed when the almost all of the *cos* DNA is bound; non-specific binding to the pBR322 fragment occurs at the same high IHF concentrations.

constant for the formation of A as 1.0×10^9 M^{-1} and for the formation of B, as 4.7×10^8 M^{-1} in the spermidine binding buffer. In the magnesium buffer the binding constant for the formation of A is reduced by a factor of 10 (data not shown).

A second model assumes that A is a complex containing one molecule of IHF and one *cos* fragment, that B contains 2 IHF molecules per *cos* fragment, and that B is in equilibrium with free IHF and free DNA, as follows:

$$DNA + IHF \rightleftharpoons A$$

$$A + IHF \rightleftharpoons B$$

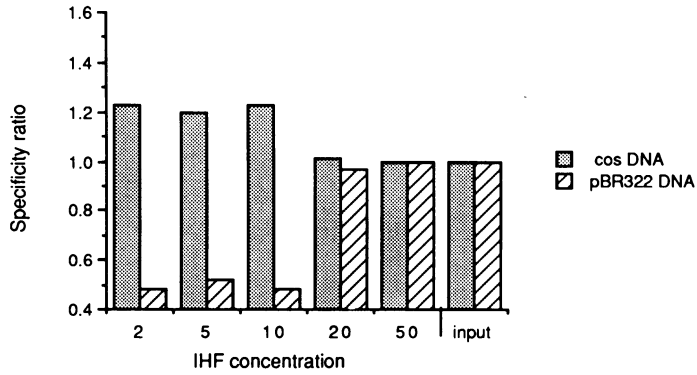

Figure 5: The specificity of IHF-DNA interactions at various concentrations of IHF.

For each of the two DNA fragments used in the experiment, shown in Fig. 4, the specificity ratio is calculated as the ratio of the (fractional contribution of that fragment to the total DNA bound) to the (fractional contribution of that fragment to the input mixture of DNA). If binding is random, the fraction of each DNA fragment bound should equal the representation in the input mixture, and the specificity ratio is equal to 1.00. At any IHF concentration, the relative deviation of the specificity ratios from 1.00 is an indication of the specificity of binding in that mixture.

The $\log_{10}$KB is the negative of the x-intercept of a plot of $\log_{10}$([B]/[A]) versus $\log_{10}$[free IHF], where now

$$[\text{free IHF}] = [\text{IHF added}] - [A] - 2[B]$$

The determination of the equilibrium binding constant for A must consider that [A] increases along with the [free DNA] but decreases with an increase in [B]. Thus,

$$\text{Log}_{10}K_A = (-1)\log_{10}K_B - (\text{x-intercept})$$

where the x-intercept now comes from a plot of $\log_{10}$([B]/[free DNA]) versus $\log_{10}$[free IHF].

Taking these considerations into account, we have calculated an equilibrium binding constant for the formation of A as 1.5×10^9 M^{-1} and for B, 1.8×10^8 M^{-1}.

Protein-Induced Bending of the DNA

The degree of retardation of band A is disproportionate to the effect expected when one molecule of IHF is added to a 398 bp fragment (28). The additional 21,800 daltons should only add about 8% (equivalent to approximately 33 bp) to the molecular weight of the DNA alone. This suggests that IHF affects the conformation of the *cos* fragment by inducing a bend near the center of the DNA molecule (40, 41).

To test if IHF bends the *cos* fragment, the 398 bp fragment was cloned in tandem, and the tandem clone was cut with a variety of restriciton enzymes to generate a population of *cos* fragments, all of the same size but with permutations of the sequence found in the original *cos* fragment. In this way the loci of the various IHF binding sites could be altered relative to the ends of the fragment. These fragments

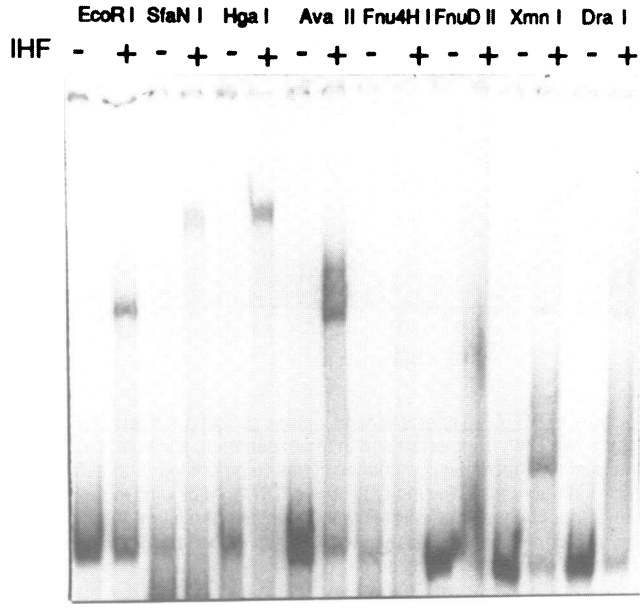

Figure 6: Complexes of IHF with permuted *cos* DNA fragments.
End-labelled fragments of each permutation of the *cos* fragment sequence, in the spermidine binding buffer, with and without added IHF, were electrophoresed at 4°C. The amount of IHF added in each case was chosen to convert some of the DNA in the mixture to IHF:DNA band A, leaving some DNA unbound. The label over each pair of lanes indicates the restriction enzyme used to prepare that DNA fragment. From left to right: *Eco*RI, *Sfa*NI, *Hga*I, *Fnu*4HI, *Fnu*DII, *Xmn*I, *Dra*I.

were used to determine whether IHF bends the DNA and to map the bending locus on the multi-site fragment.

When IHF is added to each of these permutations and the complexes are resolved by gel electrophoresis, the slowest moving permutation will be the fragment with a bend near the center of that sequence, while the fastest permutation will be the fragment with the bend closest to an end. Figure 6 shows the results of such an experiment.

Figure 6 shows an autoradiogram of eight permutations of the *cos* fragment with and without IHF. Figure 7 is a plot of densitometer scans of the eight + IHF lanes, with the location of complex A in each lane indicated by the arrow. Only a small amount of IHF was added to each fragment, leaving most DNA unbound, to ensure that the retarded complex represented complex A. To further guarantee that the IHF-*cos* complex observed was not one of the higher order complexes (B or C in Fig. 2), this experiment was also performed under conditions in which Complex B is not observed at low IHF concentrations. No effect was seen on the degree or the locus of bending (data not shown).

A plot (Fig. 8) of the mobility of the IHF-DNA complexes versus the restriction map of the tandem clone indicates a sharp bend located most closely to I1. There is a small variation in the mobility of the

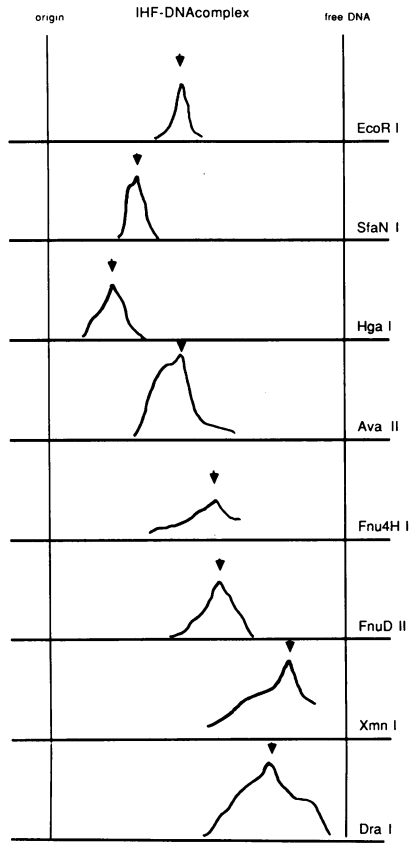

Figure 7: Densitometer tracings of permuted *cos* fragments with IHF.

The + IHF lanes in Fig. 6 were scanned by densitometry. In order to compensate for the different amounts of label in the eight preparations of the permuted *cos* fragments, the densitometer gain was adjusted for lanes *Fnu*DII, *Xmn*I and *Dra*I, to maximize intensity at the level found in the free DNA band in the corresponding - IHF lane. The arrows over the peaks of IHF-DNA complexes correspond to the location of complex A and was the point used to measure the relative mobility of the complex formed with that fragment.

DNA alone which must be due to a sequence-induced bend in the *cos* fragment itself (40,41). However, the sequence induced bend is slight compared to the dramatic alteration in mobility when IHF is bound to the fragment.

Electron Microscopy of the IHF-cos Complex

In the presence of IHF, the DNA assumed a characteristic configuration, a very acute bend near one end of the molecule. In representative fields, (Fig. 9) in the presence of IHF, 23% (88 out of 384) of the DNA molecules had the characteristic bend, while in the absence of IHF only 3.9% (8 out of 207) of the molecules had a bend of similar appearance around the expected region of the DNA fragment.

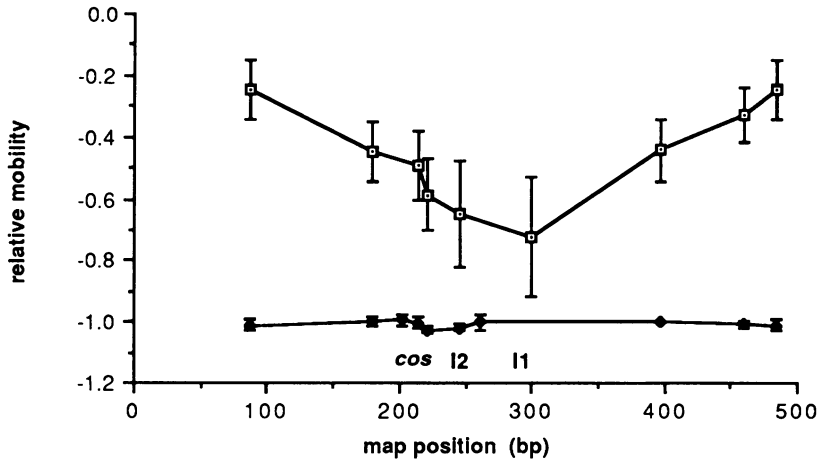

Figure 8: Relative mobility of permuted cos DNA fragments.

The graph shows the relative mobility of the permuted cos DNA fragments plotted against the restriction map of the sequence, averaged for five separate experiments, both at 4°C and at 25°C. The relative mobility is the (distance migrated by any band) divided by the (distance migrated by the *Eco*RI cut fragment without added IHF) multiplied by -1. The error bars represent the standard deviation of the measurements. Mobility of DNA without added IHF, filled diamonds; with added IHF, band A, open squares. The data points mark the following restriction enzyme sites, from left to right: *Hga*I, *Ava*II, *Hph*I, (without IHF only), *Fnu*4HI, *Fnu*DII, *Xmn*I, *Mbo*II(without IHF only), *Dra*I (with IHF only), *Eco*RI, *Sfa*NI, *Hga*I.

The 704 bp fragment contains IHF binding sites and *lacP* approximately equidistant from the two ends of the molecule; therefore, it was possible that the kink in the DNA was at the RNA polymerase binding site at *lacP*. Micrographs of fields of DNA, complexed with IHF and RNA polymerase confirmed that the two proteins bind to different ends of the DNA molecule (data not shown). In addition, another DNA fragment from pWP14, lacking *lacP* and extending from the *Hind*III site adjacent to the *Hind*II site (Fig. 10) in the pUC9 polylinker to the *Pvu*II site, was also used. Electron micrographs of this shorter fragment incubated with IHF showed the characteristic bend in the DNA in about the middle of the molecule, thus indicating that the bend is not occuring at *lacP* (data not shown).

The contour lenghts of a total of 235 distinct molecules were measured; 102 of these molecules have definite, characteristic bends. In order to determine the position of the bend in these molecules, the DNA contour length of the shorter arm to the bend was divided by the total length of the DNA fragment and multiplied by 704 (the total length of the DNA molecule in base pairs). Since the orientation of the *Hind*II lambda *cos* fragment in pWP14 is known, it is possible to calculate the lambda coordinate where the bend occurs. A histogram of the bend position is shown in Figure 10. The points in the histogram cluster around the lambda coordinates 76 to 110; the average bend position is coordinate 90±19.

The average length of the measured DNA molecules was calculated to determine if the binding of IHF appreciably changes the length of the DNA. The average length of the 102 bent molecules is

245.9±13.0 nm; the average length of the unbent molecules is 246.3±11.6 nm, whereas the average length of all molecules is 246.1±12.2 nm. Hence, the binding of IHF to the DNA does not appear to significantly shorten the DNA. The calculated length of a 704 bp fragment of B-DNA is 239 nm (assuming a rise of .34 nm per base pair).

DISCUSSION

We have shown that *E. coli*'s IHF forms complexes with a *cos* DNA fragment of bacteriophage lambda. Three bands of IHF-DNA complexes are well resolved by polyacrylamide gel electrophroesis. The formation of these complexes occurs at IHF concentrations which reasonably represent the availability of IHF within the cell, and at concentrations two orders of magnitude lower than needed to protect specific cites on *cos* DNA from nicking by DNase (22). The equilibrium binding constants for the formation of the IHF-*cos* DNA complexes are as strong as for the binding of IHF to *attP* of lambda (42). The addition of IHF to *cos* DNA produces an altered conformation which gel mobility retardation and electron microscopy show to be a sharp bend near site I1.

I1 is the strongest IHF-binding site (22), but none of the IHF-binding sites around *cos* perfectly matches the consensus sequence (20, 21). Even the two overlapping matches at the strongest site differ from the consensus by one and two base pairs. *In vitro* mutagenesis work in two laboratories (42,43) has suggested that alteration of the central adenines (positions -3 and -4), the central thymines (postions +3 and +4) or the adjacent guanine (+5) is sufficient to disrupt binding *in vitro* and function *in vivo* at *attP*. Yet around *cos* those changes do not seem to be as disruptive. One of the two I1 matches, I1A, has A not T at position +3, and the other, I1B has T not G at position +5. I2 also has a substitution for the G at +5, but footprinting results indicate that binding is weaker at I2 than at I1. Perhaps the flanking sequences around the consensus make significant contributions to IHF binding. Experiments with site-directed mutagenesis around the IHF binding sites of IS1 suggest that this is so (Pierre Prentki and David Galas, personal communication).

Two simplified models were presented for the formation of complexes in bands A and B in order to calculate an equilibrium binding constant for A, and also for B. Modeling B as either 1:1 or 2:1 complex generates reasonable equilibrium binding constants, but the implications of the two models are different. For a 2:1 complex to form at ratios of IHF to DNA much less than 1, IHF would have to bind cooperatively. Although there is no direct evidence of cooperativity, there are some hints that band B represents 2:1 complexes. Fig. 3 shows that band B increases and band A decreases when IHF concentration is increased from 0.2 nM to 2.6 nM. Secondly, band B is also observed in gel retardation experiments with a DNA fragment from pLW142 (3), which bears an 11 bp deletion encompassing I2. (L. D. Kosturko, unpublished data). Since DNase protection studies (22) show that I2 is the second strongest IHF binding consensus site near *cos*, we might expect a second 1:1 complex to utilize I2. Lastly, band B, but not band A, is sensitive to gel temperature suggesting that the presence of band B may depend on interactions (protein-protein) not needed to form a 1:1 complex (band A).

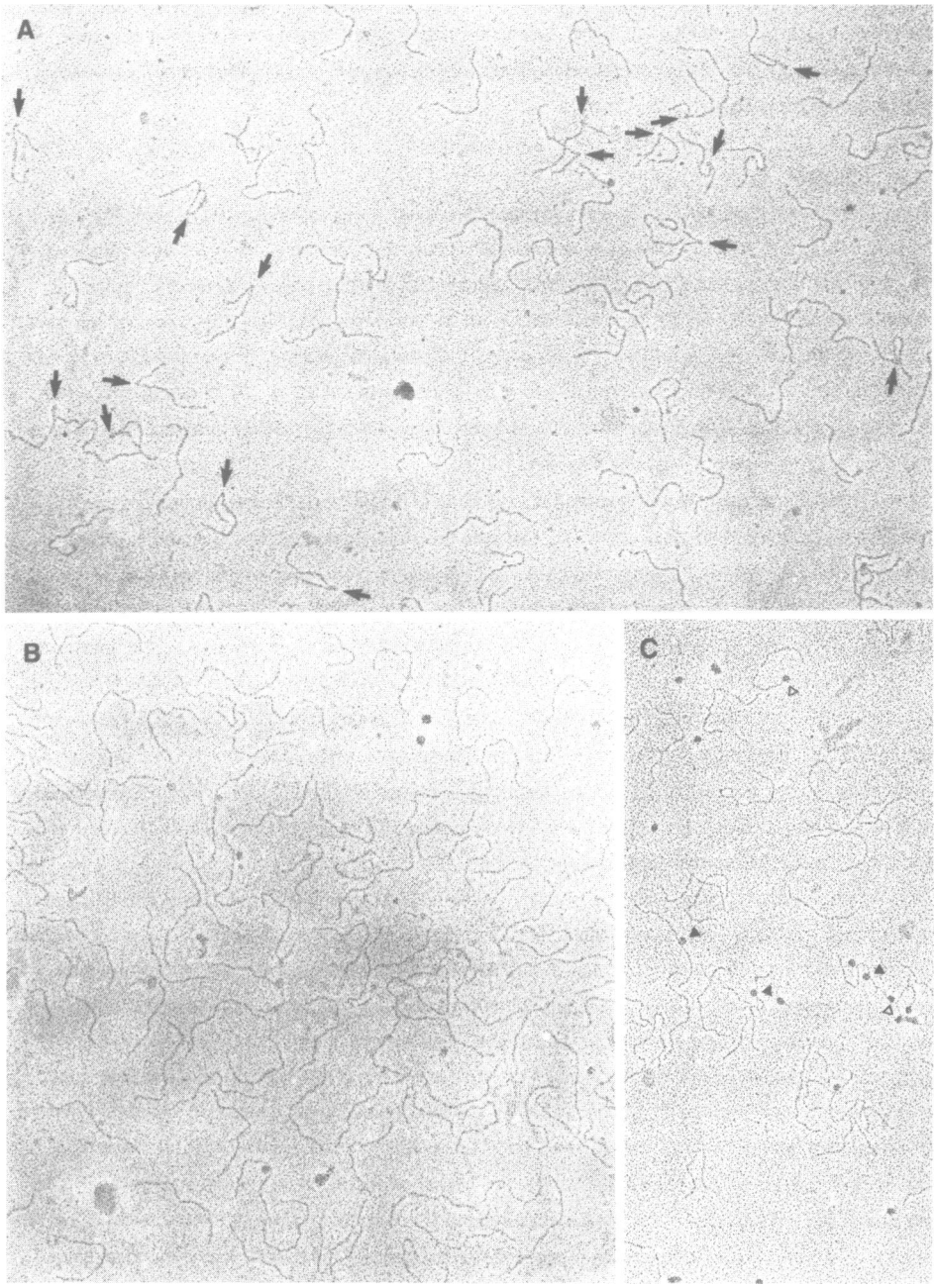
A
B
C

The resolution of this matter will require a study of the individual IHF binding sites. By cloning each site separately into a neutral background and comparing the strength of binding of each site individually, we may be able to better characterize the complexes formed with the multi-site fragment. The same experiments may also be used to determine whether IHF binds cooperatively. With other constructs we can determine whether the cooperativity requires more than one site on the DNA and how the cooperativity varies with the distance between the sites. In addition, a comparison of the footprint of the regions protected by IHF in the DNA of band A with that of band B may help to dissect the interaction.

Since the *cos* DNA fragment has multiple sites for IHF, we might expect that IHF slides among the sites, as was found for IHF binding to afragment of pBR322 (44). Our data neither prove nor disprove sliding, but the breadth of the bending curve (Fig. 6) and the distribution of bends as observed in the electronmicroscope (Fig. 10) might be taken to indicate that IHF, though bound predominantly at I1, could slide between I1 and I2.

The results presented show that *cos* contains sequences that cause a moderate intrinsic bend in the DNA. In addition, IHF introduces near *cos* a sharp bend as determined by the variable decrease in electrophoretic mobility and by direct visualization using electronmicroscopy. The angle of the bend, ϵ (epilson), as determined by electronmicroscopy is about 140°. At the atomic level an angle, $\Delta\emptyset$, can be defined as the change in the tangents to two points in the axis of the double helix separated by a distance, Δs. The curvature (K) at the point has been defined as $\Delta\emptyset/\Delta s$ (45). Δs can be taken as the distance between two adjacent base pairs, measured from the points at which the axis of the double helix intercepts the planes formed by the base pairs, and $\Delta\emptyset$ would then be the change in orientation of one base pair plane with respect to the other. The observable angle, ϵ, is equal to the sum of the $\Delta\emptyset$ within the sequence that contributes to the angle. At the electronmicroscopic level, the number of base pairs within the curvature that forms the angle ϵ is not defined. However, from the electronmicrographs it can be estimated that no more than 40 bp are involved. Therefore, the individual average $\Delta\emptyset$ must not be smaller than 140°/40 = 3.5°.

The bend of 140° is comparable to the degree of bending produced by CAP at the *lac* promoter (46, 47). CAP binds as a 45 kdalton dimer which is twice the size of the IHF heterodimer. Molecular modeling suggests that DNA wraps around CAP, resulting in a bend (48). How IHF induces such an alteration in DNA structure remains to be elucidated.

If DNA wraps around the surface of the protein (which might explain how IHF protects segments of DNA sequence far larger than its consensus), then flanking sequences may be expected to contribute to

Figure 9: Electronmicrograph of DNA-protein complexes.
A. Representative field of IHF incubated with the 704 bp fragment of *cos*-containing DNA. The arrows indicate typical bent DNA molecules. B. Representative field of the 704 bp fragment in the absence of IHF. This field also contains DNA-bound and free molecules of λ terminase. C. Representative field of *E.coli* RNA polymerase bound to the 704 bp fragment of DNA. Binding occurs at P*lac* (filled triangle) and at the ends (open triangles).

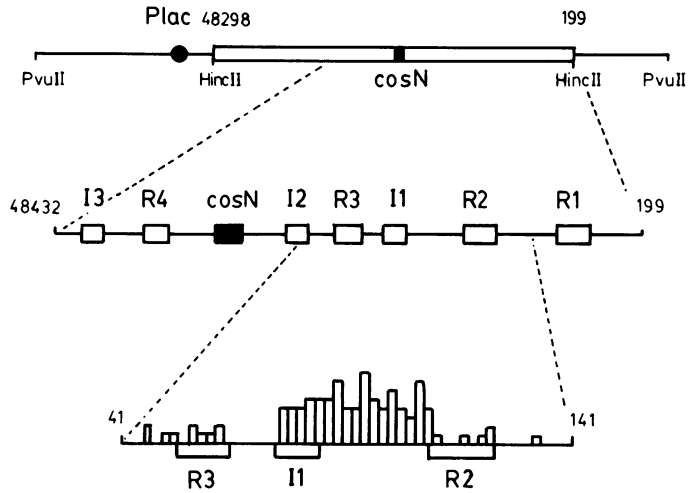

Figure 10: Position of bends in the 704 bp DNA fragment as observed by electron microscopy.
The top line shows the general features of the 704 bp DNA fragment from pWP14. In the middle line the region of the central portion of the fragment has been expanded to show the components of the *cos* region. The bottom diagram is a histogram of the distribution of the bend positions (see text). The smallest bars correspond to a frequency of 1.

the effect. Perhaps mutations introduced in flanking sequences will have a greater effect on bending than on binding itself.

What role does IHF play in lambda DNA packaging? IHF could manipulate DNA structure or bind cooperatively with terminase or both. Shinder and Gold (personal communication) have found that gp*Nul* and IHF bind cooperatively near *cos*. The strongest gp*Nul* site is R3, which is adjacent to I1. However, destabilization of terminase binding at R1 (*cos* 154) not R3, determines stringent dependency on IHF.

As a model to explain these results, we propose the following: IHF binds to I1 (and to the other sites?) and introduces a bend (s) in the DNA. The bend brings R3 closer to R2 and R1 allowing protein-protein interactions between terminase monomers at those sites stabilizing binding at the weaker sites (17).

In the absence of IHF, such an interaction is not impossible, merely less common because of the intrinsic curvature of the DNA sequence near *cos*, which could serve as a point of flexibility. Thus, in the absence of IHF, the burst size is reduced four-fold. Whether *in vivo* THF (5) is essential for the residual terminase activity in IHF-deficient cells is not known. Alterations at the I2 site (*cos*59), which would be expected to affect sequence-induced bending, result in IHF-dependent phage growth; this supports the idea that the sequences near I2 and IHF binding near I1 are interchangeable to some extent. The alteration in *Nul* which makes the *cos*59 mutant IHF-independent may produce a terminase with an enhanced

ability to interact cooperatively, able to bind to the three sites and bend the DNA without the need for auxiliary proteins.

ACKNOWLEDGEMENTS

We wish to thank: Howard Nash for his gift of IHF and for his helpful suggestions and insight; Michael Feiss and his students for the gift of plasmids and their encouragement; Martin Marinus for *dam-dcm-* cells; Asis Das and his collaborators for letting us use their cell culture facilities and for their help with the preparation of IHF; Andrew Becker and Marvin Gold for advice and encouragement; and Battista Cavalieri for technical help with electron microscopy.

This material is based upon work supported by the National Science Foundation (grant DMB 86-14196) to L.D.K. and by the Medical Research Council (Canada) to H.M.

+Present address: Department of Chemistry and Biochemistry, University of Guelph, Guelph, Ontario N1G 2W1, Canada

REFERENCES

1. Feiss, M. and Becker, A. (1983). In R. Hendrix, J. Roberts, F. Stahl and R. Weisberg (eds.), Lambda II, Cold Spring Harbor Laboratory, Cold Spring Harbor, N.Y., pp. 305-330.
2. Becker, A. and Gold, M. (1975). Proc. Natl. Acad. Sci. USA *72*:581-586.
3. Feiss, M., Widner, W., Miller, G., Johnson, G., and Christiansen, S. (1983). Gene *24*:207-218.
4. Becker, A. and Gold, M. (1978). Proc. Natl. Acad. Sci. USA *75*:4199-4203.
5. Gold, M. and Parris, W. (1986). Nucl. Acids Res. *14*:9797-9809.
6. Shinder, G., Parris, W. and Gold, M. (1988). Nucl. Acids Res. *16*:2765-2785.
7. Nash, H.A. and Robertson, C.A. (1981). J. Biol. Chem. *256*:9246-9253.
8. Drlica, K. and Rouviere-Yaniv (1987). Microbiol. Rev. *51*:301-319.
9. Weisberg, R.A. and Landy, A. (1983). In R. Hendrix, J. Roberts, F. Stahl and R. Weisberg (eds.), Lambda II, Cold Spring Harbor Laboratory, Cold Spring Harbor, N.Y., pp. 211-250.
10. Gamas, P., Burger, A.C., Churchward, G., Caro, L. and Galas, D. (1986). Mol. Gen. Genet. *202*:855-889.
11. Stenzel, T.T., Patel, P. and Bastia, D. (1987). Cell *49*:709-717.
12. Morisato, D. and Kleckner, N. (1987). Cell *51*:101-111.
13. Goosen, N. and VandePutte, P. (1984). Gene *30*:41-46.
14. Miller, H.I. (1981). Cell *25*:269-276.
15. Krause, H.M. and Higgens, P. (1986). J. Biol. Chem. *261*:3744-3752.
16. Echols, H. (1986). Science *233*:1050-1055.
17. Richet, E., Abcarian, P. and Nash, H.A. (1986). Cell *46*:1011-1021.
18. Robertson, C.A. and Nash, H.A. (1988). J. Biol. Chem. *263*:3554-3557.
19. Bear, S., Court, D. and Friedman, D. (1984). J. Virol. *52*:966-972.
20. Craig, N. and Nash, H.A. (1984). Cell *39*:707-716.
21. Leong, J., Nunes-Duby, S., Lesser, C., Youderian, P., Susskind, M. and Landy, A. (1985). J. Biol. Chem. *260*:4468-4477.
22. Xin, W. and Feiss, M. (1988). Nucl. Acids Res. *16*:2015-2030.
23. Shinder, G. and Gold, M. (1988). J. Virol. *62*:387-392.
24. Murialdo, H. (1988). Mol. Gen. Genet. In Press.
25. Miller, G. and Feiss, M. (1988). Mol. Gen. Genet. *212*:157-165.
26. Feiss, M., Fogarty, S. and Christiansen, S. (1988). Mol. Gen. Genet. *212*:142-148.
27. Granston, A.E., Alessi, D.M., Eades, L.J. and Friedman, D.I. (1988). Mol. Gen. Genet. *212*:149-156.
28. Fried, M.G. and Crothers, D.M. (1981). Nucl. Acids Res. *9*:6505-6525.
29. Garner, M. and Revzin, A. (1981). Nucl. Acids Res. *9*:3047-3060.

30. Williams, R.C. (1977). Proc. Natl. Acad. Sci. USA *74*:2311-2315.
31. Yanisch-Perron, C., Vieira, J. and Messing, J. (1985). Gene. *33*:103-119.
32. Daniels, D., Schroder, J., Szybalski, W., Sanger, F., Coulson, A., Hong, G., Hill, D., Petersen, G., Blattner, F. (1983). In R. Hendrix, J. Roberts, F. Stahl and R. Weisberg (eds.), Lambda II, Cold Spring Harbor Laboratory, Cold Spring Harbor, N.Y., pp. 519-676.
33. Parris, W., Davidson, A., Keeler, C.L. Jr. and Gold, M. (1988). J. Biol. Chem. *263*:8413-8419.
34. Maniatis, T., Fritsch, E.F. and Sambrook, J. (1983). Molecular Cloning, Cold Spring Harbor Laboratory, Cold Spring Harbor, N.Y., pp. 86-94.
35. Birnboim, H.C., and Doly, J. (1979). Nucl. Acids Res. *7*:1513-1523.
36. Maxam, A.M. and Gilbert, W. (1980). In L. Grossman and K. Modave (eds.), Methods in Enzymology, Academic Press, N.Y., Vol. 65, pp. 499-560.
37. Nash, H.A., Robertson, C.A., Flamm, E., Weisberg, R.A. and Miller, H.I. (1987). J. Bact. *169*:4124-4127.
38. Miller, H.I. and Nash, H.A. (1981). Nature *290*:523-526.
39. Fried, M.G. and Crothers, D.M. (1984). J. Mol. Biol. *172*:241-262.
40. Wu, H.-M. and Crothers, D.M. (1984). Nature *308*:509-513.
41. Koo, H.-S., Wu, H.-M. and Crothers, D.M. (1986). Nature *320*:501-506.
42. Gardner, J.F. and Nash, H.A. (1986). J. Mol. Biol. *191*:181-189.
43. Thompson, J.F., Waechter-Brulla, D., Gumport, R.I., Gardner, J., Moitoso de Vargas, L. and Landy, A. (1986). J. Bact. *168*:1343-1351.
44. Prentki, P., Chandler, M. and Galas, D.J. (1987). EMBO J. *6*:2479-2487.
45. Calladine, C.R. and Drew, H.R. (1986). J. Mol. Biol. *192*:907-918.
46. Liu-Johnson, H.N., M.R. Gartenberg and D.M. Crothers (1986). Cell *47*:995-1005.
47. Gartenberg, M.R. and Crothers, D.M. (1988). Nature 333:824-829.
48. Weber, I.T. and Steitz, T. (1984). Proc. Natl. Acad. Sci. USA *81*:3973-3977.